CrystEngComm

Accepted Manuscript

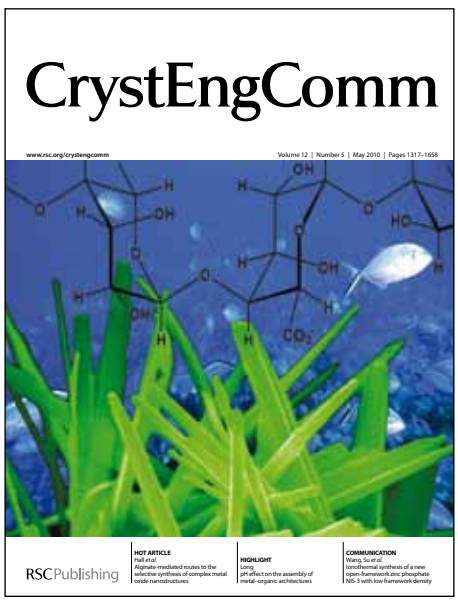

Journal Name

RSCPublishing

ARTICLE

Nano- and Micro-Hexagons of Bismuth on Polycrystalline Copper: Electrodeposition and Heavy Metal Sensing

Cite this: DOI: 10.1039/x0xx00000x

Received 00th January 2012,
Accepted 00th January 2012

DOI: 10.1039/x0xx00000x

www.rsc.org/

A. R. Rajamani,[a] Udaya Bhaskar Reddy Ragula,[a] Nikhil Kothurkar,[a] Murali Rangarajan[a]*

Hexagon-shaped bismuth nano- and micro-architectures have been electrodeposited onto polycrystalline copper electrodes from a nitrate bath at both constant current and constant potential conditions. Hexagonal geometries of varying sizes are obtained by tuning the deposition rate vis-à-vis that of a competing reaction, nitrate reduction. Nano-hexagons (100 nm to 1 μm) are obtained at 10 mA/cm^2 when the HNO_3 concentration is 0.2M or less, and with 0.4M HNO_3, hexagons of sizes up to 20 μm are deposited. The obtained hexagons are polycrystalline. Further increase in nitric acid concentration results in fused sheet-like morphologies. Increasing bismuth concentration or reducing current density results in large crystallites. Only the nanohexagons and crystallites are able to detect lead at 1 ppb. The nanohexagons show good sensitivity to detection of lead (LoD: 0.05 ppb or 0.24 nM; Sensitivity: ~ 0.75 μA/ppb) using Square-Wave Anodic Stripping Voltammetry (SWASV), and clearly distinct peaks for Pb^{2+}, Zn^{2+}, and Cd^{2+}, indicating the potential for this morphology as an electrocatalytic material.

Introduction

Bismuth, a semimetal with rhombohedral crystal structure and low melting point (271°C), has emerged over the past decade as a versatile and practical alternative to mercury[1] as an environmentally benign platform for electroanalysis. This is because of striking similarities in the physicochemical properties of the two metals, such as good electrochemical performance in both faradaic and non-faradaic measurements, excellent alloying capability with many metals, and relative insensitivity to oxygen. Further bismuth electrodes have the advantages of good mechanical stability, ease of coupling with an inert electrode substrate, and excellent electrocatalytic properties[2].

Bismuth has been electrodeposited on electrode substrates such as glassy carbon, and metals including platinum, gold, and copper[3]. It has been used for trace detection of transition and heavy metals[2]. In addition, due to its unique Fermi surface, low charge carrier density, small charge carrier effective mass, and long mean free path of charge carriers, bismuth has shown great promise as electrochromic, thermoelectric, photochromic, and magnetoresistant material[4-8]. In these applications, it has generally been recognized that the morphology and crystal structure, particularly in restricted dimensions, plays a major role in performance[2, 5, 9].

Bismuth nanostructures such as hexagons, wires and spheres, rods, tubes, cubes, branches, triangles, belts, stars, and dendrites[10-17] have been synthesized by various techniques such as chemical, photochemical, solution-liquid-solid growth, solvothermal, hydrothermal, electron-beam irradiation and lithography, thermal decomposition, vapor deposition, and electrodeposition. Among these techniques, electrodeposition has the advantages of fast synthesis, easy control of deposit sizes and morphologies at ambient conditions, flexibility for deposition on different geometries, and easy scalability compared to some of the other approaches listed above. Som *et al*[11] have reported mass synthesis of large bismuth hexagons (95-150 μm) at very high current densities (18 A/cm^2), high cathodic overpotentials (– 10V), and high concentrations (0.5M Bi^{3+} and 1M HNO_3), and have examined their thermoelectric properties and solution catalysis of reduction of 4-nitrophenol. Other work on bismuth electrodeposition from nitrate baths have investigated the mechanism of electrodeposition[18], effect of additives[19] and electrode substrates[20], and control of particle size by pulse plating[21], but there exist very few studies on the control of morphology of electrodeposited bismuth and its effect on electrocatalytic activity.

In the present work, we show that it is possible to obtain nano- and micro-hexagons of bismuth on polycrystalline copper electrodes at low current densities (1–25 mA/cm^2), low cathodic overpotentials (LSV peaks at about – 0.08 V vs.

Ag/AgCl; E_0 = + 0.317 V)[22], and low concentrations (10mM Bi^{3+} and 0.2-0.4M HNO_3) at ambient conditions. Compared with Som *et al*[11], the process consumes five-orders of magnitude less power but produces hexagons of similar sizes ranging from few hundred nanometers to tens of microns. We propose an alternate, simpler, and more cost-effective methodology to obtain similar morphologies without having to resort to high current densities, large overpotentials, and high bath concentrations, by tuning the relative rate of a competing reaction, viz. nitrate reduction. The process allows for scale up and mass synthesis. Bismuth deposits of such sizes are particularly attractive for sensor and microelectronics applications. To the best of our knowledge, there is no reported work on the electrodeposition and application of bismuth nanohexagons as electrochemical sensing platforms.

We have investigated the mechanism of bismuth electrodeposition from nitrate baths through cyclic voltammetry (CV), linear sweep voltammetry (LSV), and chronoamperometry (CA). We have electrodeposited bismuth under both galvanostatic and potentiostatic conditions. We have characterized the morphologies and crystalline nature of the deposits using high-resolution scanning electron microscopy (HRSEM) and high-resolution transmission electron microscopy (HRTEM), and selected-area electron diffraction (SAED) and X-ray diffraction (XRD) analyses, respectively. Finally, to demonstrate the effect of such controlled morphologies on electrocatalytic performance, we have studied trace detection of lead using the different morphologies. The nanohexagons give highest currents for 1 ppb lead, and show good sensitivity and linearity. We also show that simultaneous detection of lead, zinc, and cadmium could be possible using the hexagonal bismuth-modified electrode (BME) and that this morphology could be selective to these metals.

Experimental Methods

Electrochemical experiments were carried out in a standard three-electrode system using a WaveNow potentiostat (Pine Instruments) with polycrystalline copper foil (99.99% purity, Alfa Aesar, 1 cm × 2 cm) as working electrode, platinum wire (CH Instruments) as auxiliary electrode, and Ag/AgCl (3M KCl; CH Instruments) as reference electrode. Bulk electrolysis studies were carried out by using two stainless steel counter electrodes parallel to the polycrystalline copper foil under potentiostatic or galvanostatic conditions. All the chemicals used were of analytical grade. All solutions were prepared using ultrapure water (18 MΩ, Milli-Q, Millipore). In preparing the solutions, nitric acid was added until bismuth nitrate dissolved, and the solution was made up to the required concentration using ultrapure water. Before deposition the copper foil was cleaned with acetic acid, distilled water and acetone to remove the oxide layer on copper surface. For galvanostatic depositions, the deposition time was set such that the total charge passed was fixed at 7.2 C. The deposited copper foil was removed from electrolyte and then rinsed with distilled water. All experiments were carried out at ambient conditions. Surface morphology of the deposited bismuth was characterized by HRSEM using FEI Quanta FEG 200 and HRTEM analysis was carried out using JEOL JEM 2100 transmission electron microscope. The crystal structure was characterized by Powder X-ray Diffractometer (D8 Advanced, Bruker). For heavy metal detection, BME was prepared (sample A) galvanostatically at 10 mA/cm^2 for 360 s. Heavy metal solutions were prepared in 0.1M sodium acetate buffer (pH = 5.0). The metals were preconcentrated on the BME surface for 600 s at − 1.5 V, and then detected using square wave anodic stripping voltammetry.

Results

Electrodeposition of bismuth from nitrate bath is a single-step, three-electron-transfer quasi-reversible process that is diffusion-controlled. This is evinced from the results of CV (Figure S1, Supporting Information), LSV (Figures S2a-c, Supporting Information), and CA (Figures S3a-b, Supporting Information). LSV results show linear variation of peak current with respect to scan rate (Figure S2a), concentration of bismuth ions (Figure S2b), and that of nitric acid (Figure S2c). CA also shows linear variation of peak current with concentration of bismuth ions (Figure S3a), and indicates the crystal growth more likely proceeds by the progressive nucleation mechanism (Figure S3b) developed by Scharifker and Hill[18, 23].

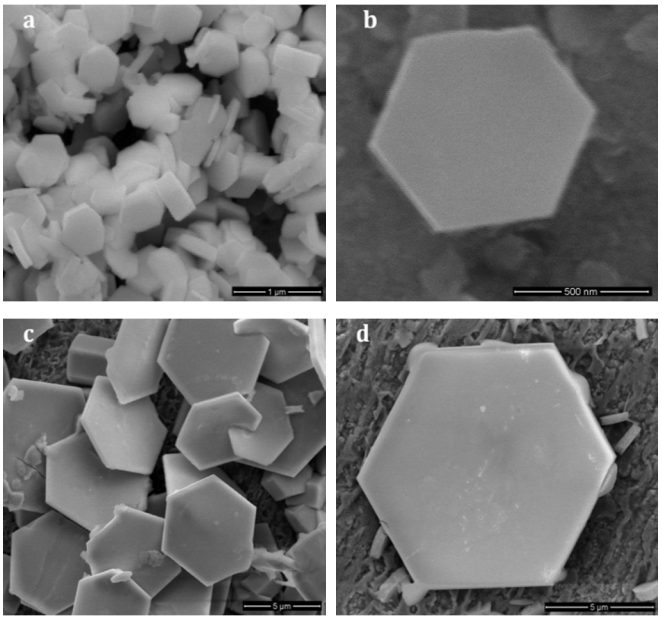

Fig. 1 SEM images of the nano- and micron-sized hexagonal bismuth deposited from 10 mM Bi3+ solution at a constant current density of 10 mA/cm2; (a), (b) Sample A (0.2 M HNO3); (c), (d) Sample B (0.4 M HNO3)

Further, in all the LSV curves, another competing reaction, of reduction of nitrate is observed at a peak potential of around − 80 mV, as also seen in earlier works[20]. The reaction is as follows:

$$NO_3^- + H_2O + 2e^- \rightarrow NO_2^- + 2OH^- \quad (1)$$

LSV studies were also conducted with polycrystalline copper cathode, platinum anode, and Ag/AgCl reference electrode for nitric acid solutions of different concentrations (0.2, 0.4, 0.6, 0.8, and 1.0M; no bismuth ions). The results, shown in Figure S4 (Supporting Information), reveal that nitrate reduction takes place at similar cathodic potentials as that of bismuth, and that the rate of nitrate reduction increases with the concentration of nitric acid.

Bulk electrodeposition of bismuth was performed galvanostatically (at three current densities) and potentiostatically (at – 150 mV), and for different concentrations of Bi^{3+} and HNO_3. The conditions studied are summarized in Table 1. The corresponding HRSEM images are shown in Figures S5a-j (Supporting Information). Of particular interest is the bismuth hexagons obtained at 10mM Bi^{3+} and 0.2 – 0.4M HNO_3 (samples A and B, respectively), shown in Figures 1a-d. When deposition is carried out in a bath containing 0.2M HNO_3, nanosized hexagons are obtained, with dimensions ranging from 300 nm to 1 μm, with thicknesses ranging from 30-80 nm. These hexagons form a longer-range branched morphology (tens to hundreds of microns long; Figure. S5a). At a nitric acid concentration of 0.4M, the hexagons are larger (up to 20 μm), and the longer-range branching is not seen probably because of the large size of the individual hexagons. At higher concentrations of nitric acid, the hexagonal morphology is lost and one observes an interleaved sheet-like morphology, which is probably the result of the various hexagons fusing together. It is seen that the current efficiency of deposition decreases with increasing nitric acid concentration, due to nitrate reduction. (Table 1.) The electrodeposition process used in this study also allows for mass synthesis of bismuth nano- and micro-hexagons, as well as the other morphologies obtained. This is seen from Figures S5 (c, d, e, g, i).

The effects of bismuth concentration (F, A, G) and current density (H, A, I) on the deposit morphology were studied at a fixed nitric acid bath concentration of 0.2M (Figure S6a-d). At a low bismuth concentration of 1mM, small hexagons are deposited (Figure S6a-b), though they are not as well-defined in morphology as those deposited from 10mM Bi^{3+} bath. At 20mM (G), larger unconsolidated crystallites of thickness in the range of microns are formed (Figure S6c-d). This morphology is similar to many reports in the literature[2, 20, 24]. It has been recognized to be similar to those of mercury films, and deemed suitable for electroanalytical purposes[2]. Similarly, at a low current density of 1 mA/cm^2, large bismuth-on-bismuth crystallites, which are fused agglomerates of hexagons, are seen (Figure S6e-g). At a high current density of 25 mA/cm^2, branched structures of nanometer-sized hexagons are seen (Figure S6h-j).

HRTEM studies reveal that the hexagons are crystalline in nature (Figure 2a-d and Figure S7a-b). Each hexagon is seen to be polycrystalline (Figure 2a-b inset). XRD studies (Figure 3) further confirm the good crystallinity of the deposit, indicating that the crystal structure contains predominantly the (0 1 2) plane, with (0 1 5), (1 1 0) and (0 2 4) planes also being present. It is of interest to note that both galvanostatic deposition (J) and potentiostatic deposition (A) result in deposits of similar morphologies (Figures 1a and S6k) and crystallinity (Figures 3,A and 3,J). Changing the bismuth concentration (Figure 3,G) or current density (Figure 3,H) does not change the crystallinity appreciably. However, it is seen that the nanostructures of bismuth (Figure 3, A and J) show other diffraction peaks, indicative of partial surface oxidation.

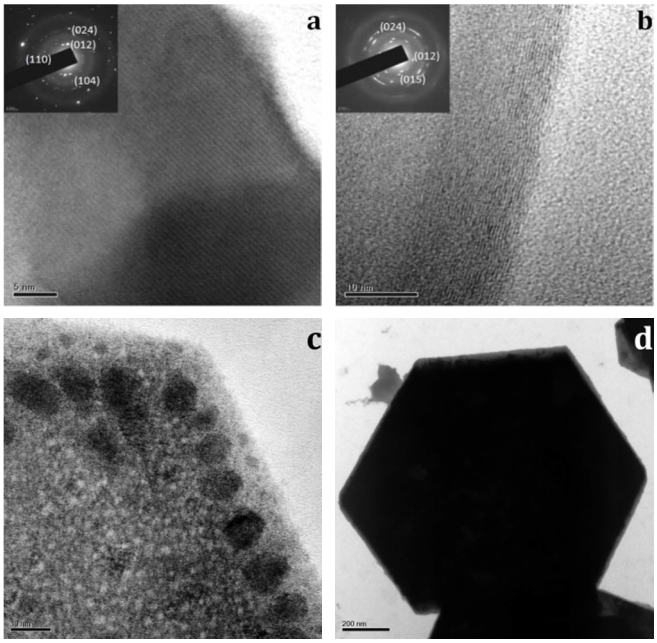

Fig. 2 HRTEM images of the hexagonal bismuth deposited from 10 mM Bi3+ solution at a constant current density of 10 mA/cm2 in (A) 0.2 M HNO3 and (B) 0.4 M HNO3; Insets are the SAED patterns. (C) Sample A showing single-crystal domains; (D) Hexagon from Sample A

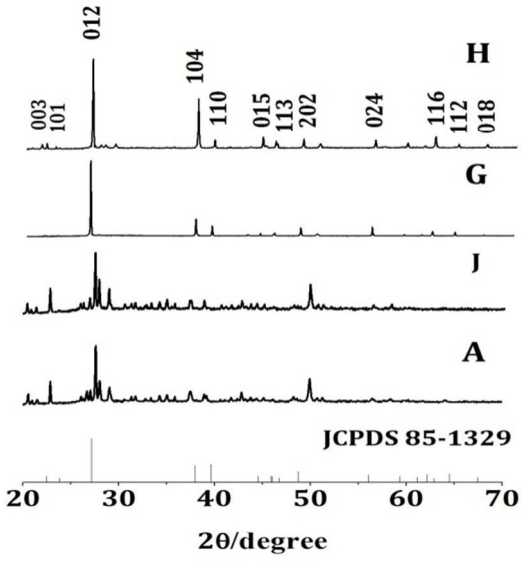

Fig. 3 XRD patterns of the different morphologies of bismuth deposited from nitrate bath. The conditions under which the different samples are deposited are given in Table 1.

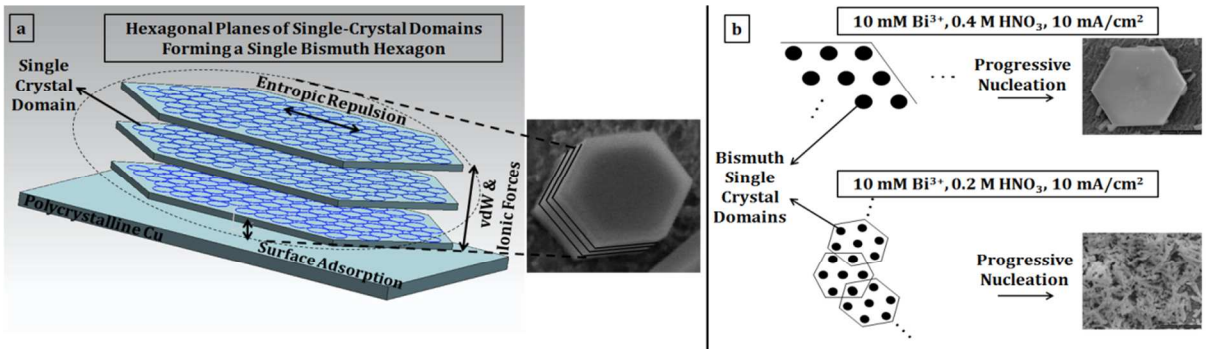

Chart. 1 Thermodynamics and kinetics of electrodeposition of polycrystalline bismuth hexagons; (a) Hexagonal geometry corresponds to minimum energy due to ionic and van der Waals interactions, surface adsorption, and entropic repulsion between single crystal domains in stacked hexagonal layers; (b) Deposition proceeds by progressive nucleation with nitrate reduction as competing reaction. At slow deposition rates, large hexagons are formed, whereas at fast rates, branched hexagons are formed.

Discussion

It is seen from the above results that nano-sized and micron-sized hexagonal bismuth plates may be electrodeposited on a polycrystalline copper from an acid nitrate bath by tuning the bismuth and nitrate concentration as well as the current density of deposition. The deposition of bismuth hexagons involves the following steps – competitive electroreduction of bismuth and nitrate ions at the electrode, progressive nucleation of bismuth on the growing crystals, surface mobility of bismuth adatoms among the growing crystals, and crystal growth. The hexagonal morphology observed may be explained (Chart 1) based on the thermodynamic and kinetic considerations of deposition and substrate effects involved.

Each hexagon may be visualized to be comprised of a number of bismuth planes held together by van der Waals forces. Each bismuth plane is comprised of single crystal domains (Figure 2c). Thermodynamically, for a given charge transferred from the cathode to the solution due to bismuth reduction, the hexagonal geometry likely corresponds to minimum total energy of the system, arising due to the ionic forces, van der Waals forces between single crystal domains in a plane and across planes, surface adsorptive forces (including at the grain boundaries of the substrate), and repulsive entropic forces due to surface confinement. However, as observed in this (Figure S4 and S5) and other studies[20], the hexagonal geometry is also dependent on the relative rates of reduction of bismuth and nitrate ions, and that of surface and interparticle diffusion[9] of bismuth adatoms.

From a kinetic standpoint, the deposition of bismuth is diffusion-limited and quasi-reversible but does not take place at limiting current. In the conditions studied in this work, nitrate reduction is a competing reaction, and its rate increases with nitric acid concentration. Increasing the supporting electrolyte concentration also increases the migratory current due to nitrate ions and hydrated protons, as seen in Figure S4. Both in turn reduce the rate of bismuth deposition. As the growth rate slows, larger hexagons are formed initially. However, further slowing down the growth rate tends to fuse these hexagons into sheets, which then fuse to form a highly interconnected sheet-like morphology. It is also of interest that while most of the hexagons are broad and disc-shaped, a few are long hexagonal cylinders. This variation might be due to the local surface conditions.

Bismuth exhibits a strong underpotential deposition[20, 25] on polycrystalline copper (as observed in Figures S2a-b) near + 50 mV (Ag/AgCl, 3M KCl). While this might have been significant if the nucleation were instantaneous, underpotential deposition has negligible effect in this system because the nucleation mechanism is predominantly progressive. At the deposition time (360 s) studied in this work, significant amount of nucleation takes place on the deposited bismuth surface itself (as is evident from the SEM images, especially in the case of branched structures). To further confirm this, potentiostatic deposition of bismuth was carried out at – 150 mV for 360 s following a one-second nucleation pulse of + 50 mV. The morphology of the obtained hexagons with and without the nucleation pulse showed no significant difference (Figure S6k-l).

It is likely that polycrystalline copper substrate too plays a significant role in determining the observed morphologies. Particularly, it is well known that the grain sizes of the substrate could have a significant effect on morphology. In this study, the substrate was used as is, without subjecting it to annealing or any other modification to change the grain sizes or crystal orientations.

Finally, it is seen that for fixed concentrations of bismuth ions and nitric acid, increasing current density favours hexagon formation. Similarly, for a fixed concentration of nitric acid and current density, lower concentrations of bismuth ions favours hexagon formation. In conjunction with the chronoamperometry results, it may be concluded that branched hexagonal structures observed in this study are likely due to progressive nucleation of bismuth on the existing deposit surfaces. Developing quantitative mechanistic models for bismuth deposition in the presence of different concentrations of bismuth ions and nitric acid, and elucidating its kinetics

requires a more detailed study of the nucleation and growth of bismuth on copper and bismuth surfaces.

Table 1 Electrodeposition of bismuth: Parameters, morphology, and sensing.

Sample	Bi^{3+} (mM)	HNO_3 (M)	CD*/ Potential	Morphology	CE† (%)	SWASV Peak Current for 1 ppb Pb^{2+} (μA)
A	10	0.2	10 mA/cm^2	Branched, Nano-sized Hexagons	100	46.59
B	10	0.4	10 mA/cm^2	Large, Micron-sized Hexagons	95.2	No peak
C	10	0.6	10 mA/cm^2	Sheets	90.4	No peak
D	10	0.8	10 mA/cm^2	Sheets	78.8	No peak
E	10	1	10 mA/cm^2	Sheets	58.7	No peak
F	1	0.2	10 mA/cm^2	Thin, Nano-sized Hexagons	-	No peak
G	20	0.2	10 mA/cm^2	Large crystallites	-	No peak
H	10	0.2	1 mA/cm^2	Large crystallites	-	11.64
I	10	0.2	25 mA/cm^2	Branched, Nano-sized Hexagons	-	43.70
J	10	0.2	– 150 mV	Branched, Nano-sized Hexagons	-	43.43

*CD: Current Density; †CE: Current Efficiency

Heavy Metals Sensing

One of the most promising applications of electrodeposited bismuth films is the detection of heavy metals, where bismuth has emerged as a practically viable alternate to mercury electrodes[2, 26-29]. A lab-on-a-chip sensor device typically contains sensing element of the size of nanometers to microns. Thus, electrodeposition of well-defined morphologies of bismuth in the nanometer to micron range is of significant interest towards the development of viable devices for trace detection of heavy metals.

Bismuth has the unique ability to form alloys with most heavy metals, which takes place during the preconcentration step for 600 s. During the square wave anodic stripping process, the deposited heavy metal (lead) is stripped even as the lead ion in solution exists in dynamic adsorption equilibrium with the electrode surface. Since bismuth is also stripped, interactions may also exist between the adsorption of bismuth and lead. A detailed theoretical treatment of the mechanism of SWASV using bismuth electrodes has been recently provided by Mirceski *et al*[30].

To examine the feasibility of the obtained morphologies of bismuth as a heavy metal sensing platform, preliminary SWASV studies were conducted with solutions containing 1 ppb of lead on BME (samples A to J). Only four samples (A, H, I, J) showed a peak (Figure S8a, b). Samples A, I, and J are nanohexagons (Table 1) while H is comprised of large crystallites, similar to other studies[2,20,24]. The hexagons recorded significantly higher currents than sample H, which is similar to what has been regarded as "the most convenient BiFE (*bismuth film electrode*) for electroanalytical purposes"[2].

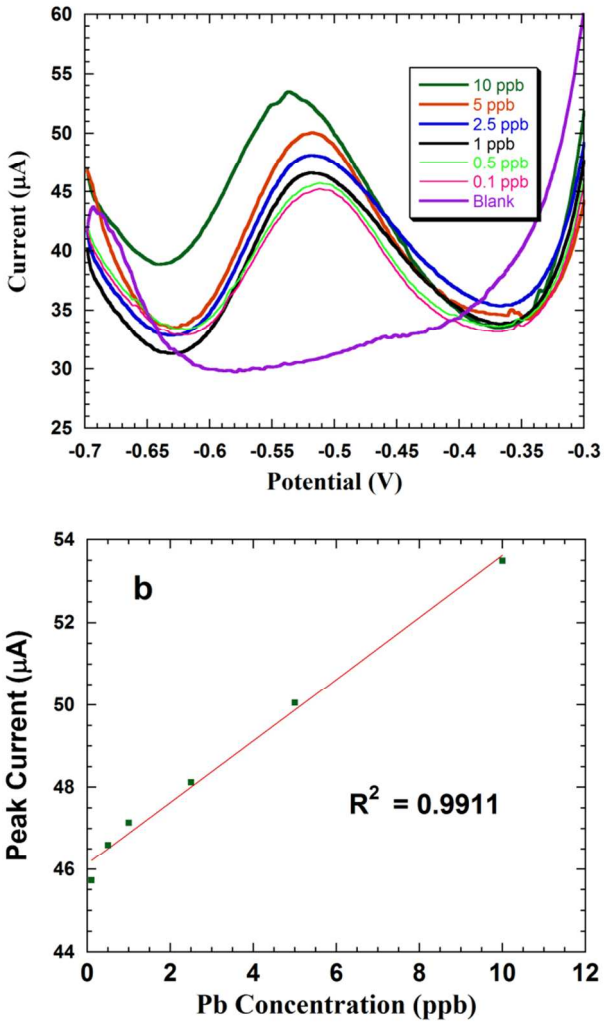

Fig. 4 (a) Square wave anodic stripping voltammograms of Pb at various concentrations 10, 5, 2.5, 1, 0.5, and 0.1 ppb on nanohexagonal bismuth-modified electrode samples A. (See Table 1 for details.) Analytes were preconcentrated at – 0.7 V for 600 s on the bismuth-modified electrode. (b) Calibration curve indicating the linear dependence of peak current on lead concentration.

Trace detection of lead was studied from 0.1 to 10 ppb on the nanohexagonal bismuth (Sample A; Figure 4). The sensor behaved in a linear fashion (I = 0.7492C + 46.135). The limit of detection was determined as 0.05 ppb (the lowest lead concentration for which the null hypothesis of equal mean signals for blank and LoD could be rejected by a two-sample Student's t-test with a one-sided alternative with $\alpha = 0.005$). SWASV studies were also conducted with solutions containing

Pb, Cd, and Zn at 10 ppm concentrations on the nanohexagonal BME (Figure 5). The separation of peak potentials for the three metals, as seen in Figure 5, is a preliminary indication of the ability of nanohexagonal bismuth (A) to selectively detect the three metals.

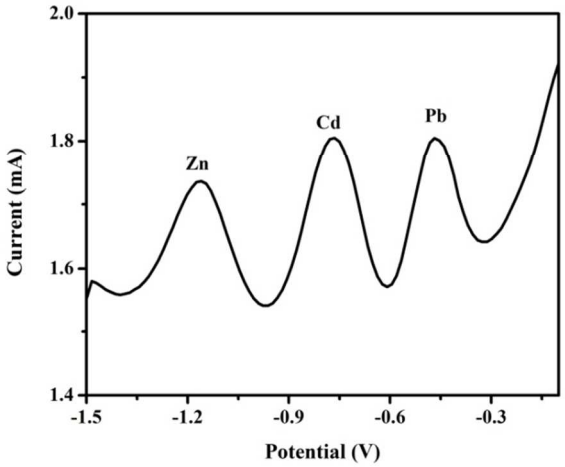

Fig. 5 Square wave anodic stripping voltammograms of Zn, Cd, and Pb at concentrations of 10 ppm each, measured on the nanohexagonal bismuth-modified electrode (sample A). Analytes were preconcentrated at – 1.5 V for 600 s on the bismuth-modified electrode.

Conclusions

In conclusion, nano- and micron-sized crystalline hexagonal morphologies of bismuth have been electrodeposited on polycrystalline copper from nitric acid bath at bismuth concentrations of 10mM, nitric acid concentrations of 0.2-0.4M, and constant current density of 10 mA/cm^2 or constant potential of – 150 mV. Electrodeposition of bismuth is a single-step, three-electron-transfer, diffusion-controlled process as seen from cyclic voltammetry, linear sweep voltammetry, and chronoamperometry, and follows the progressive nucleation mechanism. Nitrate reduction is a competing reaction, and its rate increases with nitric acid concentration. The formation of hexagons is likely due to the competition between attractive forces arising from surface interactions between bismuth crystallites and copper substrate, van der Waals interactions between the bismuth crystallites in different hexagonal layers, and repulsive forces arising from surface confinement and ionic repulsion, at fast growth rates determined by the rate of nitrate reduction. As the growth rate slows at higher nitric acid concentrations, the hexagons fuse to form larger sheets. Branched structures form due to progressive nucleation on the deposited bismuth surfaces. The nanohexagonal morphology is able to detect lead with excellent sensitivity (~ 0.75 μA/ppb) with a detection limit of 0.05 ppb. It also shows distinct peaks for metals such as lead, cadmium, and zinc, indicating its potential as an electrocatalytic material.

Acknowledgements

The work was supported financially by the Defence Research Development Organization, New Delhi, India. The authors are grateful to Amrita Vishwa Vidyapeetham for providing the infrastructure to carry out the work, and to Dr. Sriram Devanathan, Professor, Department of Chemical Engineering and Materials Science, Amrita Vishwa Vidyapeetham, Coimbatore, for discussions on estimating limit of detection.

Notes

[a]*Center of Excellence in Advanced Materials and Green Technologies, Department of Chemical Engineering and Materials Science, Amrita Vishwa Vidyapeetham, Coimbatore, India. Fax: +91 422 2656 274; Tel: +91 422 2685 000; E-Mail: r_murali@cb.amrita.edu*

†Electronic Supplementary Information (ESI) available: Results of electrochemical studies of bismuth deposition – CV, LSV in bismuth nitrate bath as functions of scan rate, bismuth ion concentration, nitric acid concentration, CA, nucleation mechanism studies, LSV in nitric acid solution, SEM images under different conditions of deposition, and TEM images of the obtained bismuth hexagons are provided. Preliminary results are also presented for the detection of 1 ppb lead by the various electrodeposited bismuth samples. See DOI: 10.1039/b000000x/

References

1. G. Aragay, A. Puig-Font, M. Cadevall and A. Merkoci, *J. Phys. Chem. C*, 2010, **114,** 9049-9055.
2. I. Švancara, C. Prior, S. B. Hočevar, and J. Wang, *Electroanalysis*, 2010, **22,** 1405 – 1420.
3. S. Jiang, Y.-H. Huang, F. Luo, N. Du and C.-H. Yan, *Inorg. Chem. Commun.,* 2003, **6,** 781-785.
4. F. Y. Yang, K. Liu, C. L. Chien and P. C. Searson, *Phys. Rev. Lett.,* 1999, **82,** 3328-3331.
5. F. Y. Yang, K. Liu, K. M. Hong, D. H. Reich, P. C. Searson and C. L. Chien, *Science,* 1999, **284,** 1335-1337.
6. L. Li, G. Li and X. Fang, *Journal of Materials Science & Technology,* 2007, **23,** 166-181.
7. J. S. Son, K. Park, M.-K. Han, C. Kang, S.-G. Park, J.-H. Kim, W. Kim, S.-J. Kim and T. Hyeon, *Angew. Chem.,* 2011, **123,** 1399-1402.
8. A. Imamura, M. Kimura, T. Kon, S. Sunohara and N. Kobayashi, *Sol. Energy Mater. Sol. Cells,* 2009, **93,** 2079-2082.
9. R. M. Penner, *J. Phys. Chem B.,* 2002, **106,** 3339-3353.
10. J. W. Wang, X. Wang, C. Peng and Y. D. Li, *Inorg. Chem.,* 2004, **43,** 7552-7556.
11. T. Som, A. Simo, R. Fenger, G. V. Troppenz, R. Bansen, N. Pfänder, F. Emmerling, J. Rappich, T. Boeck and K. Rademann, *ChemPhysChem,* 2012, **13,** 2162-2169.
12. M. Yang, *J. Mater. Chem.,* 2011, **21,** 3119-3124.
13. W. Z. Wang, B. Poudel, Y. Ma and Z. F. Ren, *J. Phys. Chem. B,* 2006, **110,** 25702-25706.
14. R. Boldt, M. Kaiser, D. KoÌˆhler, F. Krumeich and M. Ruck, *Nano Lett.,* 2009, **10,** 208-210.
15. R. Fu, S. Xu, Y.-N. Lu and J.-J. Zhu, *Cryst. Growth Des.,* 2005, **5,** 1379-1385.
16. Y. Ni, Y. Zhang, L. Zhang and J. Hong, *CrystEngComm,* 2011, **13,** 794-799.
17. S. Derrouiche, C. Z. Loebick and L. Pfefferle, *J. Phys. Chem. C,* 2010, **114,** 3431-3440.
18. M. L. Yang and Z. B. Hu, *J. Electroanal. Chem.,* 2005, **583**, 46-55.

19. Y.-D. Tsai, C.-H. Lien and C.-C. Hu, *Electrochim. Acta,* 2011, **56,** 7615-7621.
20. E. Sandnes, M. E. Williams, U. Bertocci, M. D. Vaudin and G. R. Stafford, *Electrochim. Acta,* 2007, **52,** 6221-6228.
21. C. N. Tharamani, H. C. Thejaswini and S. Sampath, *Bull. Mater. Sci.*, 2008, **31,** 207-212.
22. J. A. Dean, *Lange's Handbook of Chemistry*; McGraw-Hill, 1999.
23. B. Scharifker and G. Hills, *Electrochim. Acta,* 1983, **28,** 879-889.
24. B. O'Brien, M. Plaza, L. Y. Zhu, L. Perez, C. L. Chien and P. C. Searson, *J. Phys. Chem. C,* 2008, **112,** 12018-12023.
25. K. Tamura, J. X. Wang, R. R. Adžic and B. M. Ocko, *J. Phys. Chem. B,* 2004, **108,** 1992-1998.
26. F. Arduini, J. Q. Calvo, A. Amine, G. Palleschi and D. Moscone, *Trend Anal. Chem.,* 2010, **29**, 1295-1304.
27. G. Aragay and A. Merkoci, *Electrochim. Acta,* 2012, **84,** 49-61.
28. J. Wang, J. Lua, Ü. A. Kirgöz, S. B. Hocevar, and B. Ogorevc, *Anal. Chim. Acta,* 2001, **434**, 29-34.
29. S. Anandhakumar, J. Mathiyarasu, and K.L.N. Phani, *Indian J. Chem.,* 2012, **51A**, 699-703.
30. V. Mirceski, S. B. Hocevar, B. Ogorevc, R. Gulaboski, and I. Drangov*, Anal. Chem.* 2012, **84**, 4429-4436.

GRAPHICAL ABSTRACT FOR THE PAPER

Nano- and Micro-Hexagons of Bismuth on Polycrystalline Copper: Electrodeposition and Heavy Metals Sensing

A R. Rajamani, Udaya Bhaskar Reddy Ragula, Nikhil Kothurkar, and Murali Rangarajan

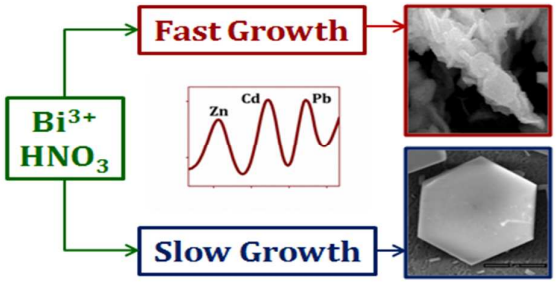

Tuning the electroreduction of NO_3^- vis-à-vis Bi^{3+} results in nano-/micro- hexagons. Nanohexagons are highly sensitive to trace detection of lead.